Pergamon

Corrosion Science, Vol. 40, No. 8, pp. 1421–1434, 1998

Printed in Great Britain.
0010-938X/98/$ see front matter

PII: S0010-938X(98)00047-X

CORROSION BEHAVIOUR OF AISI 304L AND 316L STAINLESS STEELS PREPARED BY POWDER METALLURGY IN THE PRESENCE OF SULPHURIC AND PHOSPHORIC ACID

E. OTERO,[a] A. PARDO,[a] M. V. UTRILLA,[a] E. SÁENZ,[b] J. F. ÁLVAREZ[c]

[a]Departamento de Ciencia de Materiales, Facultad de Química, Universidad Complutense, Ciudad Universitaria, 28040 Madrid, Spain.
[b]Laboratorio de Corrosión, Pontificia Universidad Católica del Perú, Lima 32, Perú.
[c]Instituto Tecnológico de Costa Rica, PO Box 159 Cartago, Costa Rica, Spain.

Abstract—The corrosion rates of AISI 304L and 316L stainless steels prepared by powder metallurgy (P/M) have been studied by continuous electrochemical methods, in different concentrations of inorganic acid solutions (sulphuric and phosphoric) at room temperature ($T = 298$ K). For comparison purposes, a simultaneous study was carried out on similar composition cast AISI 304L and AISI 316L stainless steels specially prepared for this study. For the latter part of this investigation, polarisation resistance and an intersection method were applied to obtain values for the Tafel slopes and the Stern-Geary constant B. The sintered AISI 304L and 316L stainless steels had the highest corrosion rates, these being much higher in sulphuric acid.

Subsequently, a kinetic study of the corrosion process has been carried out. The most pronounced attack was observed in those steels prepared by powder metallurgy due to a generalised mechanism of crevice corrosion taking place in the pores. On the other hand, as is already well known, the cast stainless steels generally showed a strong resistance to corrosion in the media tested.

INTRODUCTION

The corrosion resistance of sintered stainless steels is lower than that of either cast or wrought stainless steels, however, their use is mainly due to the production being economically more attractive. This is especially true when a large number of identical pieces, generally of small size and complex geometry, are produced.[1–6]

The greater chemical activity of sintered material can be reduced applying various techniques. These are mainly based on a reduction in the degree of porosity. This reduction can be achieved through the control of the sinterisation environment, dust injection moulding (PIM), passivation treatments or by modification of the composition of the sintered materials (through addition of alloy elements such as Sn, Cu or Si or noble elements such as Pt, Au or Ag).[7–12]

In previous studies, the corrosion resistance of steel materials prepared by powder metallurgy (P/M) has been compared with that of cast materials in chloride solutions, nitric acid and some organic acids. The corrosion resistance of the P/M materials was always

Manuscript received 12 June 1997; in amended form 3 March 1998

lower. In the study presented here, the behaviour of both stainless steel materials is compared in two inorganic acids at different concentrations. These are sulphuric and phosphoric acids, both of which are of great importance in the chemical industry.[13–17]

EXPERIMENTAL METHOD

The work was carried out on CAST and P/M AISI 304L and AISI 316L austenitic stainless steels. Their chemical compositions are shown in Table 1.

The P/M steels were obtained as follows: 15 g of pre-alloyed powder was uniaxially compacted at 700 MPa using zinc stearate as the matrix lubricant. Green densities of 6.40 and 6.43 gcm^{-3} were obtained for AISI 304L and 316L respectively. Sintering was carried out in a vacuum furnace at 1603 K, with a vacuum pressure <0.13 Pa, for 30 minutes. The heating and cooling rate was 5 K per minute. The products had a 25 mm diameter in the form of 4.9 mm thick discs. The density of the sintered P/M materials are 6.90 g cm^{-3} for the AISI 304L and 7.03 g cm^{-3} for the 316L (densities of 87.3% for AISI 304L and 87.9% for AISI 316L of the theoretical dense value, respectively). The size and characteristics of the pores correspond to the standard in a commercial powder metallurgic product. This is prepared in the appropriate conditions starting from the dust of stainless steel, the process of compacting and the corresponding sintering. The pores as usual present a certain irregularity in size and form. In these circumstances it is impossible to adjust the pore to a uniform model (e.g. spherical), nor does it allow to contribute data of this size, unless it is a statistical average.

The cast stainless steels were prepared by smelting two 40 kg ingots, of the desired compositions, in an induction furnace. The products were machined into specimens $15 \times 15 \times 4$ mm.

Solutions of the inorganic acids were prepared using 1, 25 and 50% concentrations by weight and the experiments were carried out a constant temperature of 298 K.

A three-electrode cell was used for electrochemical measurements. Flash welding was applied to connect the working electrode, which was the chosen steel, and the copper cable. The connection was placed in a glass mould and a resin, resistant to acids, was added in order to adhere the connection to the glass mould. The counter electrode was platinum (exposed area 1 cm^2) and the reference was a saturated calomel electrode (SCE). The exposed area of the working electrodes was 2.0 cm^2. An AMEL potentiostat, model 551, incorporating a 567 model function generator and a 500 model recorder, was used to measure and record the results.

Table 1. Chemical composition of the stainless steels.

	COMPOSITION ELEMENTS/wt%							
MATERIAL	C	Si	Mn	Cr	Ni	Mo	P	S
CAST 304L	0.018	0.83	0.76	18.4	11.0	0.01	0.006	0.004
CAST 316L	0.011	0.75	0.14	17.1	12.9	2.33	0.007	0.006
304L P/M	0.017	0.62	0.05	18.2	11.5	–	0.024	0.007
316L P/M	0.023	0.82	0.18	16.3	13.8	2.15	0.018	0.007

A potential of ± 10 mV above the corrosion potential (scanning rate 2 mVs^{-1}) was applied for different testing times to calculate the polarisation resistance (R_p), according to the standard ASTM G 59. The R_p of a corroding electrode is defined as the slope of a potential E against a current density i plot at the corrosion potential E_{corr}. From the R_p, the corrosion current density (i_{corr}) can be calculated.

The Tafel slopes were established from the active region of the corresponding anodic and cathodic curves. They were plotted by a ramp of ± 100 mV to the signal generator with a polarisation rate of 4 mVs^{-1}. When R_p was known the Stern-Geary equation was applied to obtain the current density ($i_{corr} = B/Rp$), where B is a combination of the anodic and cathodic Tafel slopes. The total test time was 360 hours. Duplicate specimens were used in each test to evaluate reproducibility. The corrosion rate (V_{corr}) was determined using Faraday's Law (ASTM G–102). The equivalent weight, which is introduced into the equation for calculating the corrosion rate, is taken from the ASTM G102 standards. It is in this table that the term "equivalent weight" is being applied. The value for both AISI 304 and AISI 316 is 25.12. Finally, the kinetic laws governing the corrosion were calculated for each experiment. The term "kinetic law" refers to the mathematical function, which relates the mass loss with time.

EXPERIMENTAL RESULTS AND DISCUSSION

Phosphoric acid results

Figure 1a shows the variation with time of the corrosion potential E_{corr} for the steels AISI 316L P/M and for CAST 316L. In the case of the power metallurgical steel, it can be seen that E_{corr} is quickly established. Figure 1b shows the variation in the corrosion potential as a function of the period of exposure and different concentrations of acid for the P/M and CAST 304L stainless steels, demonstrating that E_{corr} is only established at high acid concentrations. This is probably because under these conditions rapid and extensive dissolution of the passive layer is effected, while at lower concentrations partial dissolution (unstable passivity), with preferential attack on certain more active zones of the film, is found. In the case of the P/M product, and due to circumstances that will be discussed at a later stage, the material is found in an active state throughout the test. This is due to the greater surface area being exposed to the solution and applies for all the concentrations of acid tested.

Figure 2 presents the evolution with time of current density for the specific types of steels tested. In general, the current density increases with increasing acid concentration. The values of current density obtained for those steels prepared by powder metallurgy are an order of magnitude higher than those found for the same steels prepared by smelting, thereby confirming that the former are found in an active state in this medium. A greater resistance to the corrosion can be observed when comparing AISI 316L P/M (Figure 2a) with AISI 304L P/M (Figure 2b).

Figure 3 shows the corrosion rate V_{corr} calculated using the data of Figure 2 as a starting point and expressed as weight loss per unit area plotted against time. In every case, the behaviour is in accordance with linear kinetics. The low values of V_{corr} and the corresponding shallow slopes calculated for the cast stainless steels confirm that these materials are found in a passive state throughout the test, at least for the 1 and 25 wt% concentrations of acid. In contrast, values of V_{corr} for P/M steels were found to be two orders of magnitude greater and is reflected in the values obtained for the slopes of the

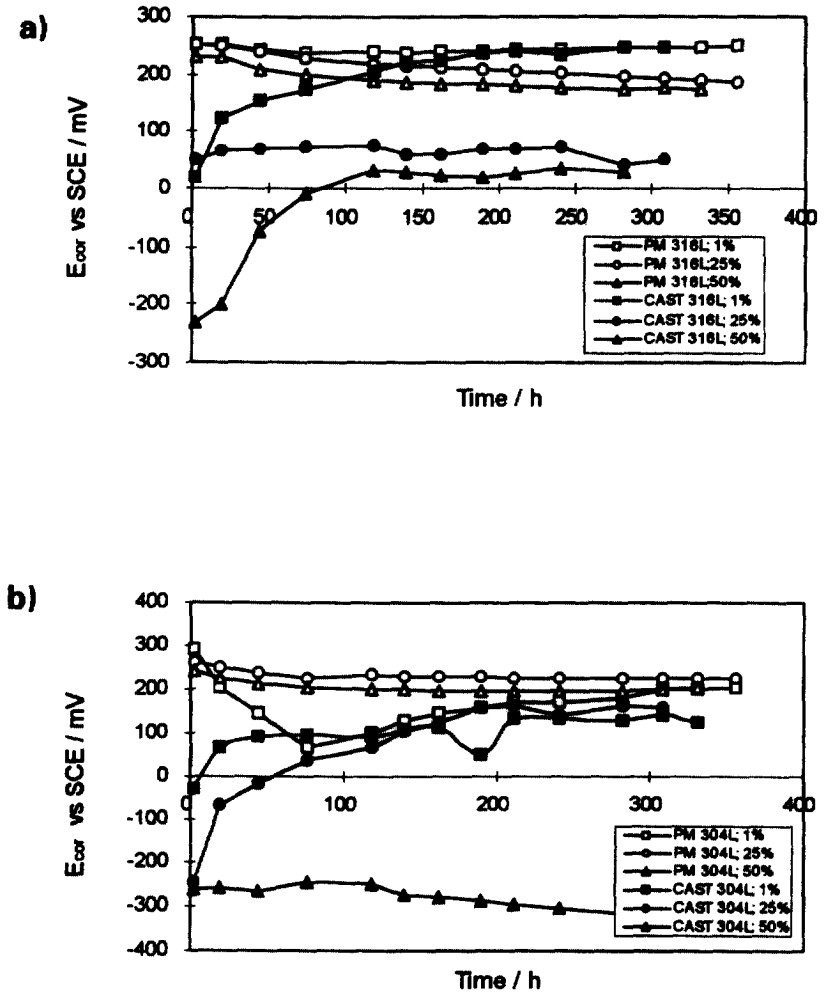

Fig. 1. Variation of the corrosion potential (E_{corr}) with time in phosphoric acid; a) P/M and CAST 316L; b) P/M and CAST 304L.

calculated kinetic laws. Similarly, it can be observed that the same steels prepared by powder metallurgy undergo generalised corrosion in the solutions tested. It can be clearly demonstrated that the AISI 304L P/M steel (Figure 3b) shows a corrosion rate which is approximately double that of the AISI 316L P/M steel (Figure 3a).

Table 2 presents the Stern-Geary constant B, where B is a combination of the anodic and cathodic Tafel slopes (b_a, b_c), and the polarisation resistance R_p of the various steels in the test solutions. The difference in magnitude between the high values of R_p in the cast materials and the low values found for those prepared by powder metallurgy again confirms that the latter are found in an active state throughout the test.

Table 3 shows the calculated kinetic laws for all the tests ($y = a + bt$). The "y" coordinate represents the mass loss in units of mg cm^{-2}. The slope (b) has units of mg cm^{-2} h^{-1}, therefore the smaller its value the greater will be the resistance of the material

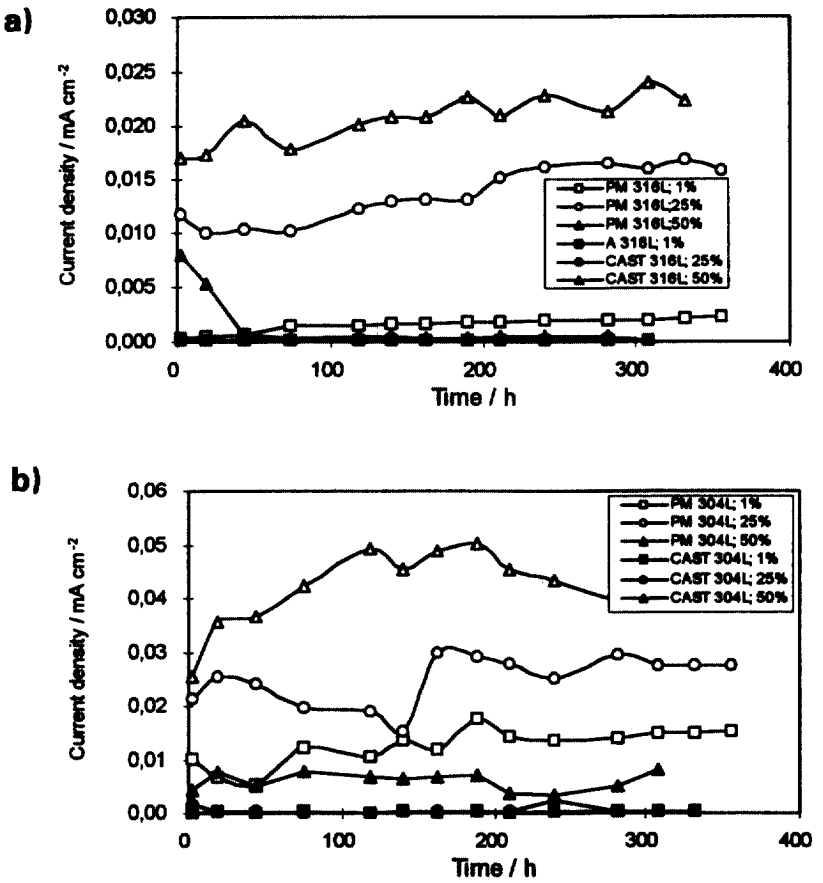

Fig. 2. Variation of the current density (i_{corr}) with time in phosphoric acid; a) P/M and CAST 316L; b) P/M and CAST 304L.

to the corrosion in this medium with respect to time. In all the cases, the kinetics complies with a linear behaviour. As expected for the solutions tested at room temperature, the kinetic constants calculated for the cast steels are low. This indicates an overall good resistance against the corrosion. Comparing these results with those obtained for the P/M steels, differences up to two orders of magnitude may be observed. In general, the slopes of the calculated equations become steeper with an increase in the acid concentration. The slopes obtained with the P/M materials show the most significant increases.

Sulphuric acid results

In this solution the P/M steels demonstrate an elevated corrosion rate. For this reason it was possible to perform measurements and provide data only for the first 50 hours of testing. On the other hand, it was possible to complete all testing with the same steels prepared by casting due to their greater corrosion resistance.

Figure 4 shows the variation in the corrosion potential E_{corr} with the period of

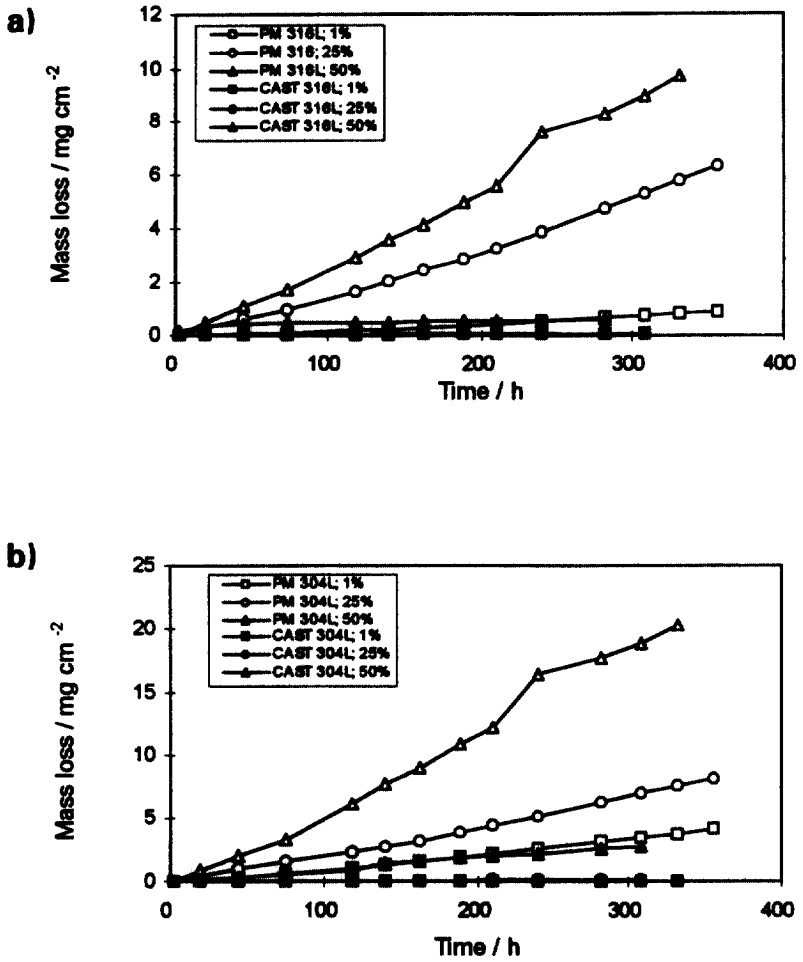

Fig. 3. Variation of the corrosion rate (mass loss) with time in phosphoric acid; a) P/M and CAST 316L; b) P/M and CAST 304L.

Table 2. Variation of the Stern-Geary constant B and the polarisation resistance R_p for the materials tested in phosphoric acid.

	Acid concentration					
	1 wt%		25 wt%		50 wt%	
MATERIAL	Rp/Ω	B/mV	Rp/Ω	B/mV	Rp/Ω	B/mV
304L PM	442	24	219	26	104	20
316L PM	3154	21	325	21	202	20
CAST 304L	1.7×10^5	95	1.0×10^5	53	616	32
CAST 316L	3.3×10^5	105	1.2×10^5	62	0.3×10^5	83

Table 3. Kinetic laws of the corrosion process calculated in phosphoric acid.

MATERIAL	Acid concentration/ wt%	Kinetic law t > 0 h y/mg cm^{-2}; t/h	r
304L P/M	1	$y = -0.29 + 0.01\,t$	0.990
	25	$y = -0.23 + 0.02\,t$	0.995
	50	$y = -0.55 + 0.06\,t$	0.990
316L P/M	1	$y = -0.09 + 2.6 \times 10^{-3}\,t$	0.988
	25	$y = -0.29 + 0.02\,t$	0.991
	50	$y = -0.25 + 0.03\,t$	0.999
CAST 304L	1	$y = -1.3 \times 10^{-3} + 1.8x10 - 4\,t$	0.999
	25	$y = -2.8 \times 10^{-3} + 4.6x10 - 4\,t$	0.940
	50	$y = -0.04 + 8 \times 10^{-3}\,t$	0.993
CAST 316L	1	$y = -1.7 \times 10^{-3} + 2.1x10 - 4\,t$	0.997
	25	$y = -3.7 \times 10^{-3} + 2.8x10 - 4\,t$	0.994
	50	$y = -0.01 + 6.3 \times 10^{-3}\,t;\ t < 45\,h$	0.997
		$y = 0.39 + 5.5 \times 10^{-4}\,t;\ t > 45\,h$	0.996

exposure. In general one can observe that the potential is established more quickly in this test solution. Similarly, it can be seen how, under the same test conditions, the steels prepared by sintering show a greater (more noble) corrosion potential than those prepared by powder metallurgy. This is due to the greater stability of the passive layer in the smelted materials.

Figure 5 presents the evolution of the current density with time for the various types of steel. Regarding the P/M steels, testing was suspended beyond 50 and 70 hours for the concentrations of 50 and 25 wt% acid respectively, due to the dissolution of the samples.

For longer time periods, the current densities were so high that the detection limit of the apparatus was exceeded, causing the destruction of the sample. Once more the AISI 304L (Figure 5b) compared with the AISI 316L (Figure 5a) stainless steel proved to be less resistant to the corrosion. This is true for both the CAST and P/M steels. In all the materials tested in sulphuric acid, it can be seen that the current density increases significantly when the concentration of acid is above 25 wt%.

Figure 6 shows the corrosion rates calculated using the data of Figure 5 as a starting point and expressed as weight loss per unit area plotted against time. From the comparison of the data obtained it can be concluded that the steels prepared by powder metallurgy show an elevated corrosion rate, much higher than the corresponding value for the CAST materials. The AISI 316L P/M stainless steel (Figure 6a) shows a better behaviour against corrosion in this medium than the AISI 304L P/M steel (Figure 6b). At H_2SO_4 concentrations of 1 wt%, weight losses are already 70 times higher than the corresponding values for AISI 316L P/M.

Figure 7 presents the microstructures of the CAST AISI 316L and 316L P/M stainless steels exposed to 50 wt% H_2SO_4 during 48 hours. The difference of the degree of attack on the individual steel types can be observed.

Table 4 shows the Stern-Geary constant B and the polarisation resistance R_p of the various materials in the test solutions under the conditions in which it was possible to

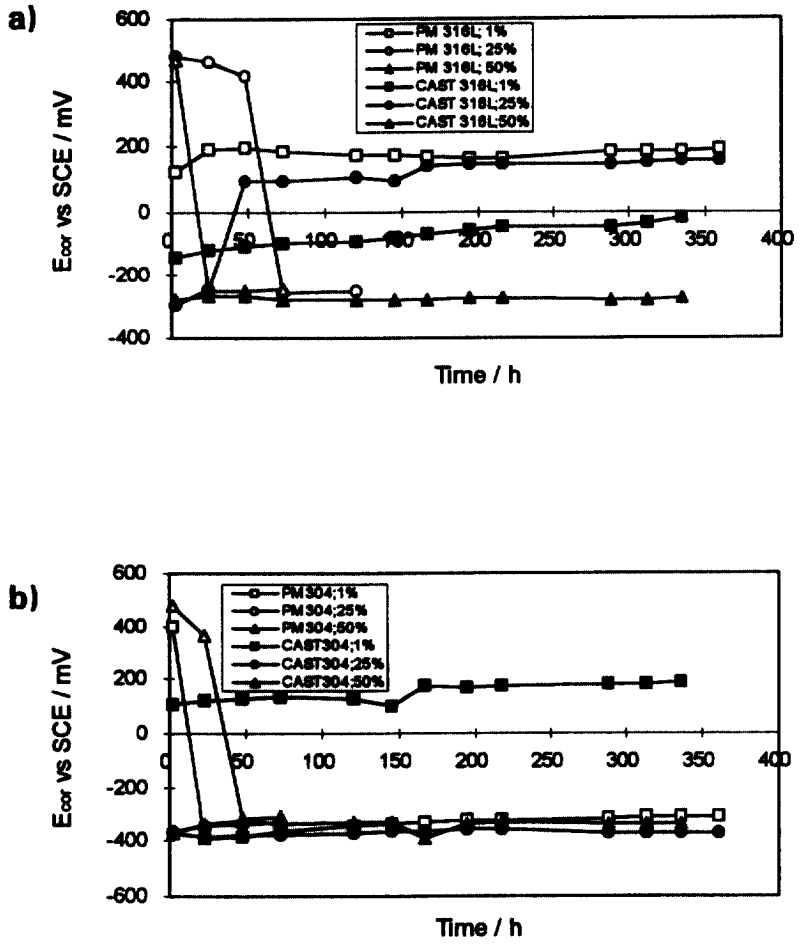

Fig. 4. Variation of the corrosion potential (E_{corr}) with time in sulphuric acid; a) P/M and CAST 316L; b) P/M and CAST 304L.

Table 4. Variation of the Stern-Geary constant B and the polarisation resistance Rp for the materials tested in sulphuric acid.

	Acid concentration					
	1 wt%		25 wt%		50 wt%	
MATERIAL	Rp/Ω	B/mV	Rp/Ω	B/mV	Rp/Ω	B/mV
304L PM	334	28	3	22	82	20
316L PM	3253	35	259	26	17	38
CAST 304L	319538	102	17	10	11	12
CAST 316L	69957	45	32882	53	5	15

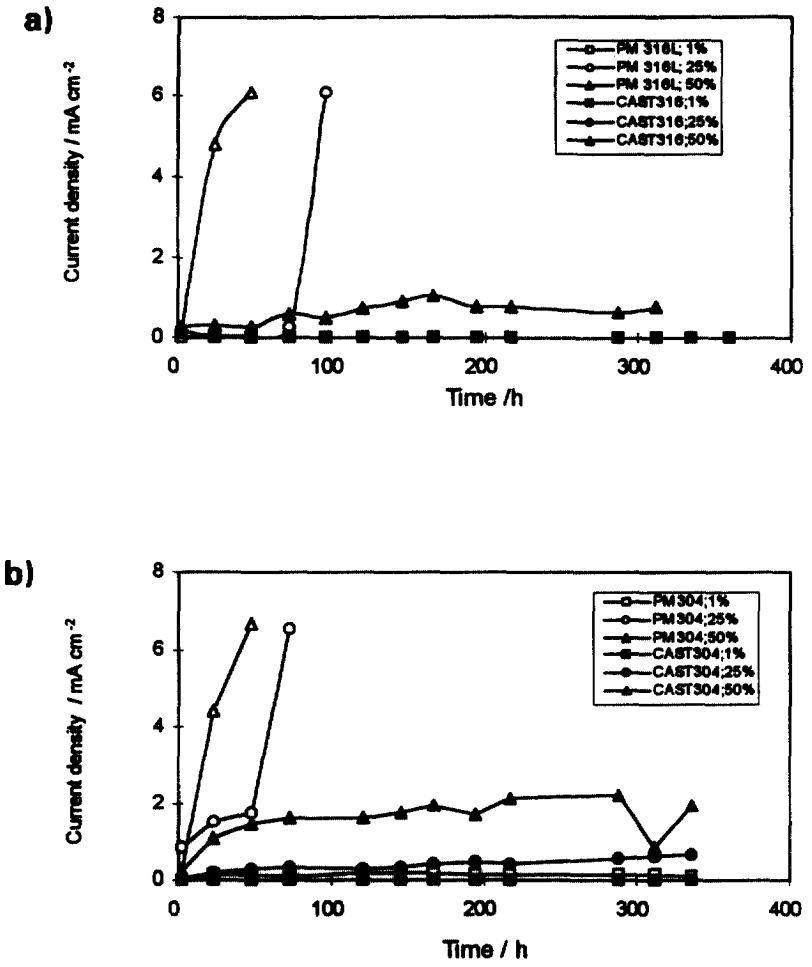

Fig. 5. Variation of the current density (i_{corr}) with time in sulphuric acid; a) P/M and CAST 316L; b) P/M and CAST 304L.

complete the testing. Due to the lack of values in the literature for this type of materials, Tafel slopes were calculated.

Table 5 shows the calculated kinetic laws for all the tests with the same "y" coordinate and slope definition as mentioned for the previous set of results. Again, the smaller the slope value the greater will be the resistance of the material to the corrosion in this medium with respect to time. As can be seen, in all cases the kinetic behaviour is linear. For the P/M stainless steels exposed to 25% and 50 wt% H_2SO_4 the kinetics have only been calculated for time periods less than 72 and 48 hours respectively. This results in a change from linear kinetics to potentials whose exponent increases with increasing acid concentration.

Corrosion mechanisms

The mechanism proposed to justify the high corrosion kinetics observed in the P/M products is based on attack through crevice corrosion. This starts in the pores and

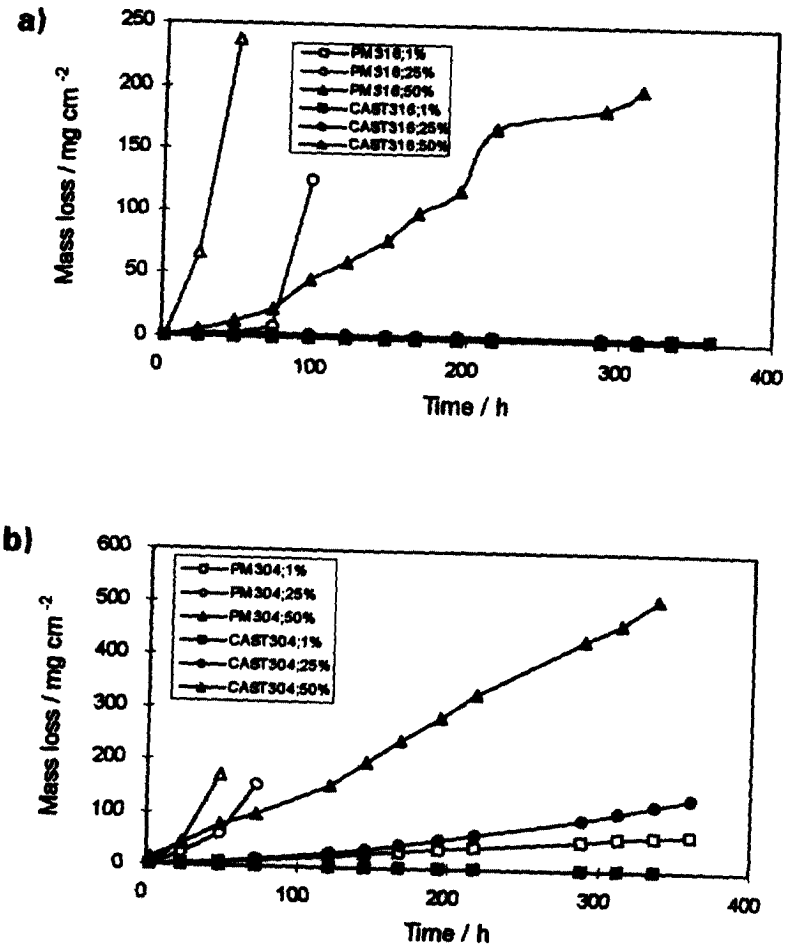

Fig. 6. Variation of the corrosion rate (mass loss) with time in sulphuric acid; a)P/M and CAST 316L; b) P/M and CAST 304L.

becomes more widespread, progressively moving to the interior of the material throughout the period of exposure to the aggressive solution. The form of this type of attack is a function of the susceptibility of the alloy and of the aggressivity of the dissolution, while its intensity depends on the geometry of the cracks, their dimensions and specific electrochemical factors.

Passive alloys, such as the stainless steels analysed in this study, have a greater tendency to be affected by cracking corrosion than alloys with a more active behaviour.

The nucleation and propagation of the phenomenon is associated with the creation and development of localised solutions, different to the general solution, in the interior of the crack. The presence of pores favours the setting-up of differential airing cavities and the differential concentration of protons. In the pore, which acts like a crack, a point is reached where oxygen is used up while the ventilated zones of the surface have immediate access to this gas.

Under these conditions, the corrosion potential in the ventilated zone of the crack

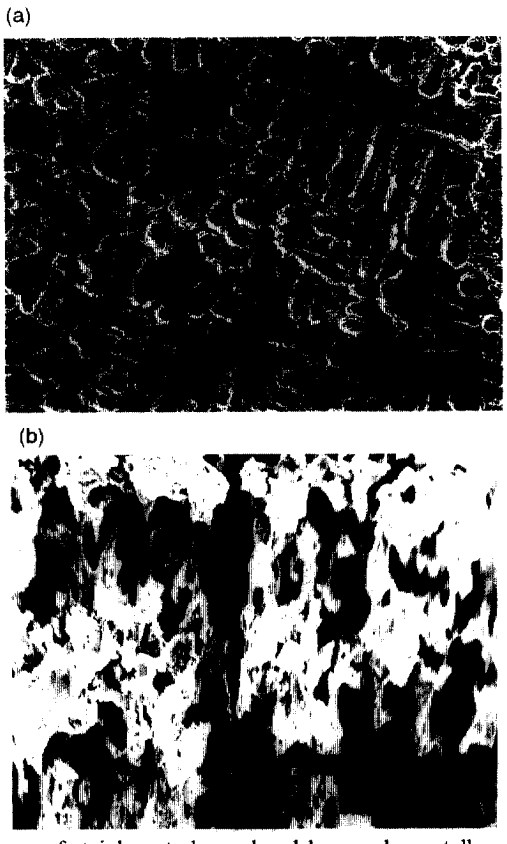

Fig. 7. Microstructures of stainless steels produced by powder metallurgy exposed to 50 wt% H_2SO_4 solution during 48 hours; a) CAST AISI 316L, b) AISI 316L P/M.

Table 5. Kinetic laws of the corrosion process calculated in sulphuric acid.

MATERIAL	Acid concentration/ wt%	Kinetic law t > 0 h y/mg cm^{-2}; t/h	r
304L P/M	1	$y = -2.29 + 0.20\,t$	0.998
	25	$y = 0.23\,t^{1.5}$; t < 72 h	0.996
	50	$y = 7 \times 10^{-3}$ t2.7; t < 48 h	0.990
316L P/M	1	$y = -0.06 + 7 \times 10^{-3}\,t$	0.997
	25	$y = 0.04\,e^{0.08t}$; t < 76 h	0.938
	50	$y = 0.02\,t^{2.4}$; t < 48 h	0.996
CAST 304L	1	$y = -3.3 \times 10^{-3} + 1.3 \times 10 - 4\,t$	0.994
	25	$y = 0.01\,t^{1.6}$	0.996
	50	$y = 0.07\,t^{1.5}$	0.998
CAST 316L	1	$y = -3.8 \times 10^{-3} + 2.6 \times 10 - 4\,t$	0.877
	25	$y = 0.23\,t^{0.5}$	0.995
	50	$y = 0.08\,t^{1.3}$	0.996

is maintained above that of passivation and consequently the passive layer remains stable. In contrast, active conditions within the pore are found and active-passive cells are set up.

The initiation of cracking corrosion in the powder metallurgical materials analysed is produced through the release of metallic ions, principally chromium, in the interior of the pore and this leads to conditions of acidification as a result of the hydrolysis reaction:[18-20]

$$Cr^{3+} + 3H_2O \leftrightarrow Cr(OH)_3 + 3H^+$$

The geometry of the crack is, in the majority of situations, the controlling factor, which governs the resistance to this type of corrosion.

The crevices or cracks can be classified according to the degree of narrowness and depth, taking into account the efficiency in generating phenomena of crevice corrosion. In the case of a powder metallurgical material, where the aperture (pore) is very narrow, the volume of electrolyte to be deoxygenated and acidified is reduced. This results in an initiation of attack which is both more rapid and severe. When the concentration of protons is sufficiently high to place the material within the corrosion zone of the Pourbaix diagram, the passive layer is dissolved and the attack commences down towards the interior of the pore. Just how this takes place is shown in Fig. 8a and 8b.

At a later stage, the attack advances towards the interior of the powder metallurgical materials by means of basic mechanisms. On the one hand, this is as a consequence of the functioning of the active-passive cells, already described, between the regions with a stable passive layer and the central region of the original metallic dust particles in contact with the electrolyte with an elevated local concentration of protons representing the active component. On the other hand, the attack progresses by means of the fusion between the original dust particles through a mechanism of crevice corrosion as shown in Figure 8c.

The final result is the general disintegration of the material mainly due to the selective attack through the crevices of the regions where solid phase soldering had taken place between the particles during smelting (Figure 8d). The effect of an increase in local pressure due to the formation of gaseous hydrogen, a result of the cathodic reaction of a reduction in protons, also contributes to the disintegration.

CONCLUSIONS

(1) The stainless steel AISI 316L P/M shows a greater resistance to corrosion than AISI 304L P/M in both solutions, but these are always appreciably lower than for the cast stainless steels.

(2) The corrosion rates in phosphoric acid are lower than those calculated for sulphuric acid. In the latter, total dissolution of the powder metallurgical samples is produced in acid concentrations of 25 and 50 wt% within 100 hours.

(3) In the powder metallurgical steels, the attack is initiated primarily in the pores. This is due to the mechanism of hydrolysis where there is a local concentration of protons. This leads to the dissolution of the passive layer and the functioning of active-passive cells between the interior of the pore and the surface of the metal. The attack is complemented by the mechanisms of crevice corrosion. These circumstances explain the high corrosion rates observed in the powder metallurgical materials.

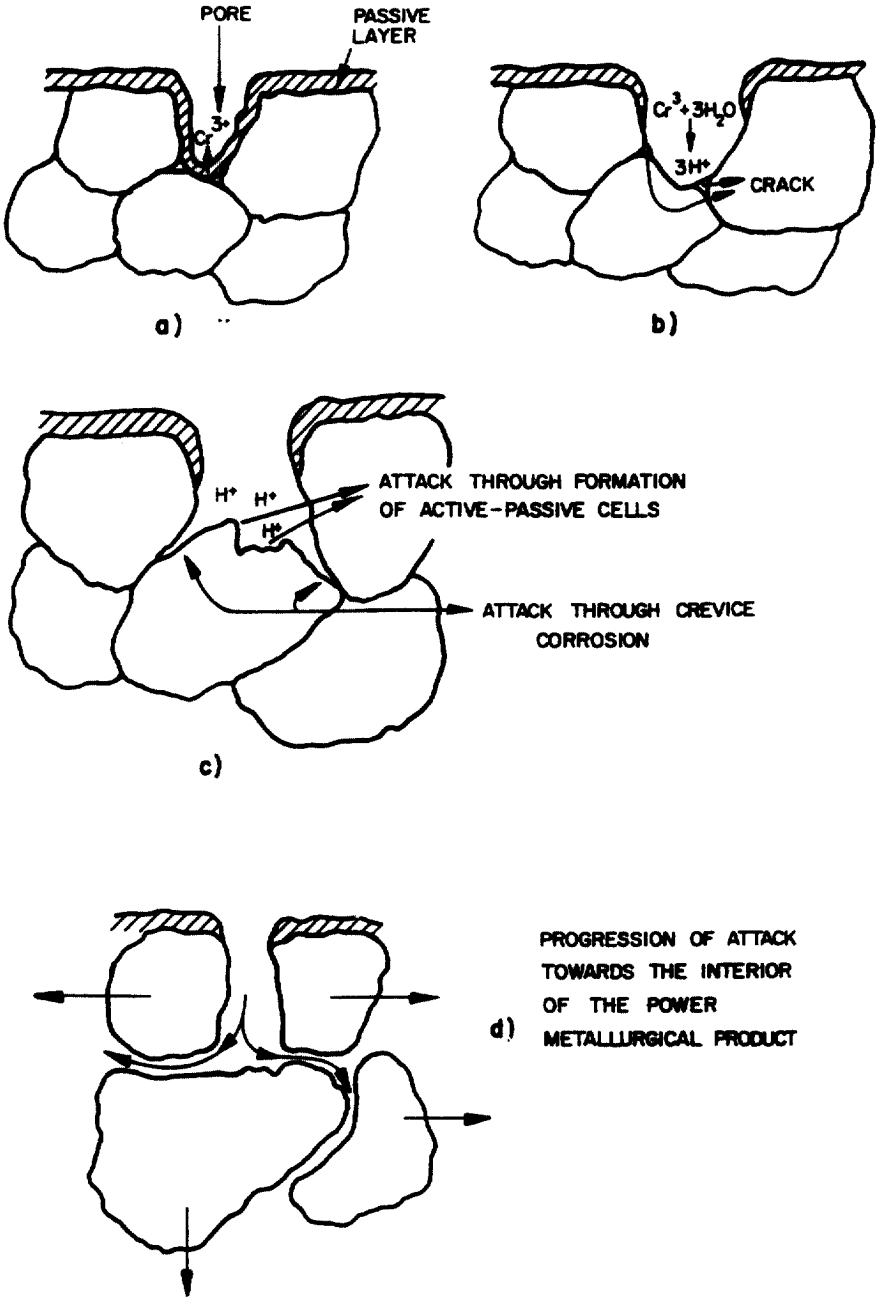

Fig. 8. Corrosion mechanisms of stainless steels produced by powder metallurgy.

Acknowledgements—The authors express their gratitude to the Comisión Interministerial de la Ciencia y Tecnologia (CICYT) for their financial support of this work (Project MAT 96-0917).

REFERENCES

1. Lindshog, P. *Metal Powder Report*, 1992, **47,** 32.
2. Ambs, H. D., *Proc. Advances in Powder Metallurgy*, MPIF, Chicago, Illinois, USA, **3**, 89, 1991.
3. Eisenmann, M., Fisher, A., Leismann, H. and Sicken, R., *Modern Developments in Powder Metallurgy*, 1988, **21,** 637.
4. Gold, R., *Precision Metal*, 1982, **3,** 31.
5. Agapiou, J. S., Halldin, G. W., De Vries, M. F., Journal of Engineering for Industry *Transactions ASME*, 1989, **110,** 339.
6. Chiaverini, V. and Jeszensky, G., *Proc. Conf. Advances in Powder Metallurgy*, MPIF, San Francisco, California, USA, **5**, 359, 1992.
7. Angelini, E., Bianco, P., Rosalnino, F., Rosso, M. and Scavino, G., *Proc. Conf.* 12th International Corrosion Congress, NACE, Houston, Texas, USA, 1154, 1993.
8. Peled, P. and Itzhak, D., *Corros. Sci.*, 1991, **32,** 83.
9. Johansson, A., Arnberg, L., Gustafson, P. and Savage, S., *Proc. Conf. Advances in Powder Metallurgy*, MPIF, Pittsburgh, Pensilvania, USA, 287, 1990.
10. Sharon, A., Melman, N. and Itzhak, D., *Proc. Conf. Advances in Powder Metallurgy*, MPIF, San Francisco, California, USA, 399, 1992.
11. Lal, S. and Upadhyaya, G. S., *Journal of Material Science*, 1989, **24,** 3069.
12. Fedrizzi, L., Molinari, A., Deflorian, F., Ciaghi, L. and Bonora, P. L., *Corrosion*, 1990, **46,** 672.
13. Otero, E., Pardo, A., Sáenz, E., Utrilla, M. V. and Pérez, F. J., *Revista de Metalurgia*, 1993, **29,** 356.
14. Otero, E., Pardo, A., Utrilla, M. V., Sáenz, E. and Pérez, F. J., *Materials Characterization*, 1995, **35,** 145.
15. Otero, E., Pardo, A., Sáenz, E., Utrilla, M. V. and Hierro, P., *Corrosion Science*, 1996, **38,** 1485.
16. Otero, E., Pardo, A., Sáenz, E., Utrilla, M. V. and Pérez, F. J., *Canadian Metallurgical Quarterly*, 1997, **36,** 65.
17. Otero, A., Pardo, A., Utrilla, M. V., Pérez, F. J. and Merino, C., *Corrosion Science*, 1997, **39,** 453.
18. Lee, T. S., Kain, R. M. and Oldfield, J. W., Proc. Conf. Corrosioń 83, paper 69, NACE, Houston, 1983.
19. Kain, R. M. *Corrosion*, 1984, **40,** 313.
20. Kain, R. M. *Mater. Perforrm.*, 1984, **33,** 205.